Molecular dynamics simulations of AOT-water/formamide reverse micelles: Structural and dynamical properties

Matías H. H. Pomata,[1] Daniel Laria,[1,2] Munir S. Skaf,[3] and M. Dolores Elola[1,a)]
[1]*Departamento de Física, Comisión Nacional de Energía Atómica, Avenida Libertador 8250, 1429 Buenos Aires, Argentina*
[2]*Departamento de Química Inorgánica, Analítica y Química-Física e INQUIMAE, Facultad de Ciencias Exactas y Naturales, Universidad de Buenos Aires, Ciudad Universitaria, Pabellón II, 1428 Buenos Aires, Argentina*
[3]*Institute of Chemistry, State University of Campinas-UNICAMP, P.O. Box 6154, Campinas, São Paulo 13084-862, Brazil*

(Received 31 July 2008; accepted 16 November 2008; published online 23 December 2008)

We present results from molecular dynamics simulations performed on reverse micelles immersed in cyclohexane. Three different inner polar phases are considered: water (W), formamide (FM), and an equimolar mixture of the two solvents. In all cases, the surfactant was sodium bis(2-ethylhexyl) sulfosuccinate (usually known as AOT). The initial radii of the micelles were $R \sim 15$ Å, while the corresponding polar solvent-to-surfactant molar ratios were intermediate between $w_0=4.3$ for FM and $w_0=7$ for W. The resulting overall shapes of the micelles resemble distorted ellipsoids, with average eccentricities of the order of ~ 0.75. Moreover, the pattern of the surfactant layer separating the inner pool from the non-polar phase looks highly irregular, with a roughness characterized by length scales comparable to the micelle radii. Solvent dipole orientation polarization along radial directions exhibit steady growths as one moves from central positions toward head group locations. Local density correlations within the micelles indicate preferential solvation of sodium ionic species by water, in contrast to the behavior found in bulk equimolar mixtures. Still, a sizable fraction of $\sim 90\%$ of Na^+ remains associated with the head groups. Compared to bulk results, the translational and rotational modes of the confined solvents exhibit important retardations, most notably those operated in rotational motions where the characteristic time scales may be up to 50 times larger. Modifications of the intramolecular connectivity expressed in terms of the average number of hydrogen bonds and their lifetimes are also discussed. © *2008 American Institute of Physics*. [DOI: 10.1063/1.3042275]

I. INTRODUCTION

The study of the properties of the water-in-oil microemulsions commonly known as reverse micelles has been a focus of interest over the past 50 years.[1] Reverse micelles represent polar nanodroplets dispersed in apolar solvents and stabilized by surfactants. These self-assembled structures are formed when mixtures of water, surfactants, and nonpolar solvents are combined at the appropriate concentrations, leading to a confined polar liquid phase lying at the interior of the aggregates. The resulting size of these droplets, which are usually portrayed in terms of a spherical-like nucleus with radius R, depends on the polar-phase/surfactant relative concentration. For the particular case of aqueous reverse micelles, this parameter is usually referred to as the water-to-surfactant molar ratio,

$$w_0 = [H_2O]/[AOT]. \quad (1)$$

In most cases, and based on simple geometrical considerations, a linear relationship is found between R and w_0.

The joint effects of the prevailing confinement, combined with the strong interactions between the polar solvent molecules and the surfactant head groups, generally of the Coulomb type, lead to nanophases, whose structural and dynamical characteristics may differ dramatically from those observed in more conventional, i.e., bulk-like environments.[2] As such, reverse micelles have been used as size-controlled microreactors for a variety of chemical reactions in solution. In addition, they have also been extensively used to facilitate the incorporation of sparingly soluble molecules into nonpolar phases. Moreover, the analysis of chemical reactivity within reverse micelles is relevant to many areas of biochemistry, given their resemblance to more complex biological vesicles.

From the experimental point of view, the structure and dynamics of aqueous micelles have been studied using a wide variety of techniques. The list includes fluorescence,[3,4] NMR,[5–7] neutron and x-ray scattering,[8–11] quasi-elastic light scattering, and infrared[12,13] and terahertz[14] spectroscopies, to cite a few relevant examples. On the other hand, and from a theoretical perspective, these systems have also been investigated, normally resorting on computer simulations incorporating different degrees of molecular detail to model the polar and non-polar phases and the surfactants as well.[15–31]

Compared to the previous body of available results regarding aqueous reverse micelles, the information about mi-

a)Electronic mail: doloreselola@gmail.com.

TABLE I. Parameters used to set up the initial configurations of the reverse micelle systems. R is the radius of the initial core for each micelle, n_{AOT}, n_W, n_{FM}, and n_{CHEX} are the numbers of AOT, water, formamide, and cyclohexane molecules composing the simulated systems. L is the simulation box length and t is the temporal length of the simulation experiment.

Micelle	w_0	R/Å	n_{AOT}	n_W	n_{FM}	n_{CHEX}	L (Å)	t (ns)
RMW	7	14	82	574	···	2296	75.39	5
RMWF	5.5	14	66	183	183	2347	76.31	5
RMF	4.3	14	60	···	260	2380	75.43	5

croemulsions containing nonaqueous polar phases is much less abundant. One of the first studies of reverse micelles in which the aqueous phase was replaced by polar solvents such as glycerol and formamide was reported in 1984.[32–34] Since then, formamide trapped within reverse micelles has been extensively analyzed, becoming a classical example for nonaqueous trapped phases. Consequently, we will briefly summarize in what follows some relevant information about these systems: (i) The analysis of vibrational spectra of formamide/AOT reverse micelles performed by Riter *et al.*[35] suggests that the hydrogen bond structure of formamide would appear significantly less perturbed by the restricted environment than that of water within similar micelles. However, their solvation dynamics measurements indicate that formamide in the central nucleus is nearly immobilized, exhibiting a much more dramatic departure from its bulk dynamical behavior than water does. (ii) In addition, Shirota and Segawa[36] found that the solvation time constants of formamide in micelles are between two and three orders of magnitude slower than those of pure formamide; moreover, they found a strong dependence of the solvation time with w_0: the solvation dynamics of formamide becomes faster as w_0 increases, a well-recognized trend already observed in aqueous reverse micelles.[16,37,38] (iii) Laia *et al.*[39] performed light scattering experiments that would indicate that in formamide/AOT micelles the polar head groups (PHGs) are poorly solvated by formamide, leading to a strong association between the AOT polar heads and Na^+ counterions, resulting in an overall electrically neutral interfacial region. (iv) Finally, Correa *et al.*[40] employed Fourier transform infrared and NMR techniques to explore the solubilization of formamide and its aqueous solutions by AOT in reverse micelles. Their results indicate that formamide interacts strongly with the Na^+ counterions, while preserving the HB network found in the bulk phase. Moreover, by comparing chemical shifts of AOT in these micelles they concluded that the stronger preferential solvation of Na^+ by formamide would be counterbalanced by a preferential solvation of the AOT's sulfonate group by water.

Given the inherent complexities of these multicomponent systems, it would be desirable to support at least part of the previous assertions with the results obtained from theoretical approaches. In an effort to provide additional elements pertaining to the microscopic description of nonaqueous micelles, we present in this paper the results from molecular dynamics (MD) experiments performed on water-formamide/AOT reversed micelles immersed in cyclohexane. The analysis presented here includes equilibrium structural and dynamical properties. In all cases, we present a comparison between the micellar behaviors and those exhibited by the corresponding bulk mixtures, which have been thoroughly investigated over the whole concentration range using a variety of experimental techniques[41–44] and computer simulations.[45–50] However, the micellar sizes investigated in this work are still smaller than those utilized in the vibrational spectroscopy analysis[35] and solvation dynamics experiments,[36] which impairs a direct comparison between our simulations and these experimental results. Yet, our simulations do provide some physically meaningful insights that contribute to the molecular level understanding of these systems. In particular, we find that (a) the micelles exhibit a considerable degree of asphericity and interfacial roughness, irrespective of the polar-phase composition; (b) a drastic reduction in the number of hydrogen bonds relative to the bulk phase; and (c) an inhomogeneous distribution of the cosolvents in the micelle interior. Interestingly, we find that the overall effects of the confinement upon the dynamics of the polar phases are reflected into a general slowing down involving translational and reorientational motions and hydrogen bond dynamics.

The organization of the paper is as follows: Sec. II describes the interaction potentials and some technical details concerning the implementation of the simulations. Structural results, spatial correlations between different species, and polarization fluctuations of the inner polar pools are discussed in Sec. III. Sections IV and V include all the dynamical information that we extracted from our simulations. The main conclusions of the paper are summarized in Sec. VI.

II. SYSTEMS STUDIED AND SIMULATION DETAILS

Three micellar environments were investigated: in two of them, the polar phases are composed of pure water (RMW) and formamide (RMF); in addition, we also examined a third system (RMWF), in which the inner pool consisted of an equimolar mixture of the two solvents. In all cases, the ionic surfactant is sodium 1,4-bis(2-ethylhexyl)-sulfosuccinate (AOT) and the external organic phase is composed of cyclohexane (CHEX). Table I summarizes the relevant parameters concerning size and composition of the three simulated micelles.

For the particular case of RMW, the initial radius (R =14 Å), the amount of water (n_W=574), and the relative concentration (w_0=7) were chosen such as to coincide with those of the system denoted as RM82 in the previous analy-

sis performed by Abel *et al.*[23] In order to facilitate the comparison, the rest of the micelles investigated were also prepared with similar initial radii. The amounts of each solvent n_i contained in the inner pools were selected by taking into account the corresponding packing as reflected by ρ_α, the density of the corresponding bulk phase,[51,50] namely,

$$n_\alpha = n_W \frac{\rho_\alpha}{\rho_W}. \tag{2}$$

Concerning the amount of surfactants, n_{AOT} in RMF, we adopted an *ad hoc* criterion based on the results from a series of preliminary simulation runs, in which we examined the stability of micelles containing increasing amounts of AOT. Our final choice, $n_{AOT}=60$, which corresponds to $w_0 \sim 4$, represented the smallest amount that would yield a stable micellar structure over the entire time span of our simulations, typically 5 ns. Once the limiting molar ratios for the two pure solvents have been established, the value of w_0 for the mixed micelle was set by a linear interpolation: $w_0=5.5$ ($n_\alpha=183$ for $\alpha=$W and FM).

With the exception of the nonpolar phase, the rest of inter- and intramolecular interactions were modeled using the CHARMM27 force field.[52] Water was described by the TIP3P model.[53] In order to reduce computational costs, we implemented a simplified model for CHEX by adopting a united-atom description for each CH_2 group. As such, each molecule comprised six sites interacting via Lennard-Jones potentials. The parameters for the usual intramolecular interactions involving bond stretching, bending, and torsional degrees of freedom were adjusted based on the GROMOS96 force field.[54,55] We remark that, with this set of parameters, we succeeded in reproducing the experimental bulk density and the C–C pair correlation functions for pure CHEX reported in Ref. 56, which employed an explicit hydrogen force field.

The simulation experiments corresponded to microcanonical runs performed at average temperatures close to $T=298$ K and average pressures of ~ 1 bar. The preparation of the systems involved a sequential procedure similar to the one described previously in Ref. 26: the inner phases of the micelles were constructed by first extracting spherical samples from previously equilibrated bulk systems containing the polar solvents and Na^+. In addition, n_{AOT} surfactants were evenly distributed around the free interfaces of the spherical samples. The initial intramolecular configurations of the surfactant tails corresponded to fully *trans*-conformers, whereas their head-to-tail vectors were oriented radially outward. Once the head groups made contact with the substrate, the surfactants were allowed to accommodate at the surface of the polar pool during a time interval of ~ 300 ps. A subsequent high-temperature equilibration period followed in which only the tails were allowed to move at temperatures ~ 500 K for about 200 ps. From then on, ambient conditions were slowly recovered by multiple velocity rescalings and the surfactant-coated polar nucleus was surrounded by the organic phase. During the final stage, the systems were equilibrated at ambient conditions along *NPT* runs, for about 0.5 ns. At the final stages, the thermostats and barostats were switched off. The production runs typically lasted 5 ns. Along these periods the overall structure of the micelles looks sufficiently stable so as to extract physically meaningful statistical averages. Long range forces arising from Coulomb interactions were treated by a particle-mesh Ewald sum procedure. The MD simulation experiments were performed using the NAMD software package.[57]

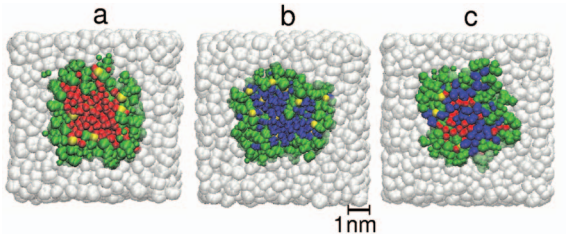

FIG. 1. (Color) Snapshots across the $z=0$ plane of the reverse micelle systems studied: (a), (b), and (c) correspond to RMW, RMF, and RMWF respectively. The red, blue, yellow, and green colors correspond to water, formamide, sodium ions, and AOT molecules, respectively. The cyclohexane molecules filling the simulation cubic box are rendered in gray.

III. STRUCTURAL PROPERTIES

The first aspect that we will examine concerns the overall shape of the micelles. Figure 1 shows the snapshots of typical configurations of the three types investigated.

Following the analysis of Ref. 23, a quantitative estimate of the overall departure from the spherical shape can be obtained from the relative magnitude of the three principal moments of inertia of the micelles, $I_1 > I_2 > I_3$. Moreover, assuming an overall ellipsoidal geometry, the three values of I_i provide estimates for the three semiaxes a, b, and c, namely,

$$I_1 = \frac{1}{5}M(a^2+b^2),$$

$$I_2 = \frac{1}{5}M(a^2+c^2), \tag{3}$$

$$I_3 = \frac{1}{5}M(b^2+c^2),$$

where M is the total mass of the micelle. In this context, a relevant order parameter is given by the micellar eccentricity, defined as

$$e = \sqrt{1-\frac{c^2}{a^2}}, \tag{4}$$

which varies from $e \sim 0$ to $e \sim 1$, as one moves from spherical-like to elongated, needle-like, structures. In Table II, we present the results for the average eccentricity for the reverse micelles.

TABLE II. Average values and the corresponding fluctuations of the eccentricity (e) and radius of gyration (R_g) for the three micelles studied.

	RMW	RMF	RMWF
e^{inn}	0.86 ± 0.01	0.71 ± 0.02	0.69 ± 0.02
e^{AOT}	0.80 ± 0.01	0.66 ± 0.02	0.62 ± 0.02
R_g^{inn}	18.00 ± 0.14	15.12 ± 0.13	15.36 ± 0.15
R_g^{AOT}	21.19 ± 0.14	18.39 ± 0.08	19.00 ± 0.07

The superscripts "inn" and "AOT" denote, respectively, whether the internal core exclusively or the core plus surfactant molecules were considered for the calculation. The average eccentricities for the three micelles are similar in magnitude: $\langle e^{\mathrm{inn}}\rangle = 0.86$, 0.71, and 0.69 and $\langle e^{\mathrm{AOT}}\rangle = 0.80$, 0.66, and 0.62 for the RMW, RMF, and RMWF, respectively. The eccentricities for the RMW are slightly larger than those reported by Abel *et al.* in Ref. 23 [i.e., $\langle e^{\mathrm{inn}}\rangle = 0.8$ and $\langle e^{\mathrm{AOT}}\rangle = 0.7$], although we tend to believe that differences in the composition of the non-polar phase may account for these minor discrepancies. For uniform ellipsoids, the radius of gyration R_g provides an estimate of a characteristic length scale associated with the micellar size and can be directly obtained from the magnitudes of the three semiaxes, namely,

$$R_g^2 = \frac{a^2 + b^2 + c^2}{5}. \tag{5}$$

Results for R_g are also shown in Table II. Two features are worth commenting: (i) for RMF and RMWF, the magnitudes of the fluctuations in R_g^{AOT} and R_g^{inn} contrast sharply, revealing differences in the geometrical patterns that describe the two interfaces. As a result, those involving the inner-pool/head groups look more irregular than the external ones, which involve the hydrophobic tails/nonpolar phase. On the other hand, these differences practically vanish for RMW. (ii) Also note that the differences $R_g^{\mathrm{AOT}} - R_g^{\mathrm{inn}}$ provide rough estimates for the thickness of the surfactant layer (in the present cases, all results are intermediate between 3 and 4 Å). This length scale should be compared to the typical size of a fully stretched, i.e., all-*trans*, AOT hydrophobic tail, which is of the order of ~12 Å. These differences would reveal a non-negligible extent of entanglement between different hydrophobic segments and an overall tilt that deviates considerably from a radial arrangement.

Local density fields provide additional structural information involving spatial correlations in the inhomogeneous micellar environments. Assuming a spherical-like geometry for the inner pool, a reasonable choice for the origin of the reference system is the center of mass of the micelles $\mathbf{R}_{\mathrm{c.m.}}$. In Fig. 2, we present the density profiles calculated from

$$\rho_\alpha(r) = \frac{1}{4\pi r^2} \sum_i \langle \delta(|\mathbf{r}_i^\alpha - \mathbf{R}_{\mathrm{c.m.}}| - r)\rangle. \tag{6}$$

In this equation, $\langle \cdots \rangle$ denotes an equilibrium ensemble average, whereas $\mathbf{r}_i^\alpha$ represents the coordinate of the ith site of species α. The results are shown for the following species: in the polar phase, we selected Na^+ ions and the centers of mass of the solvent molecules; in the surfactants, our attention is focused on the S atoms located on the head groups and all C atoms comprising the hydrophobic tails; finally, for CHEX, all six CH_2 groups were considered.

At a first glance, three spatial domains are clearly perceptible. In the inner nucleus, say, $r \lesssim 10$ Å, the prevailing species are those corresponding to the polar solvents, while for $r \sim 25$ Å and beyond, CHEX predominates. In between, there is an intermediate region occupied by the surfactants that includes the two interfaces: the internal polar-phase/head groups and the external hydrophobic tails/CHEX. A closer

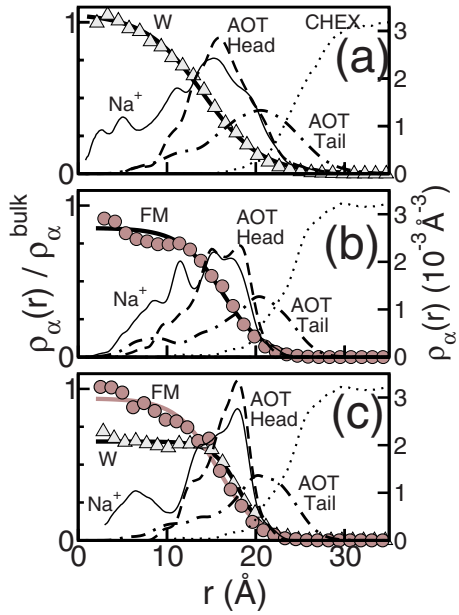

FIG. 2. (Color online) Density profiles with respect to the center of mass of the micelle core (right y-axis). Water, formamide, and cyclohexane density profiles are normalized with respect to the corresponding bulk densities (left y-axis). Panels (a), (b), and (c) correspond to RMW, RMF, and RMWF respectively (see text). The continuous thick curves are just a guide to the eye.

inspection of the profiles reveals additional details: (i) the density profiles of both polar solvents present smooth decays over relatively large spatial intervals, extending from ~10 up to 20 Å. Except for RMW, the asymptotic bulk value $\rho_\alpha^{\mathrm{bulk}} = \lim_{r\to 0} \rho_\alpha(r)$ is only marginally attained. In mixed micelles, the profiles suggest a small local enhancement of formamide near the micellar center, in detriment of water; (ii) the sodium density profiles are multimodal, with the concentration of free Na^+ near the center of the polar pool being slightly enhanced in RMW. Yet, in all cases, a sizable fraction of Na^+ ions remains associated with the anionic head groups in the interfacial region. This fraction is larger for RMF, where the fraction of Na^+ tightly bound to the head groups is approximately 0.90. (iii) No relevant differences were observed in the overall density profiles of the head groups and hydrophobic tails. In RMW the former looks Gaussian-like with a width of ~5 Å. For micelles containing FM, the profiles are somewhat more asymmetric, and some structure is also perceptible in the 15–20 Å range. (iv) The tail profiles for all three micellar environments are broad, with contributions starting from distances as short as $r \sim 7$–10 Å. These results indicate that in these small micelles the overall shapes depart markedly from a spherical geometry. Moreover, the pattern of the surfactant layer separating the polar from the nonpolar phases looks highly irregular, with a characteristic roughness comparable to the micellar radius. In passing, we remark that the irregularity in the water/surfactant interface clearly contrasts with the one observed in Faeder's simulations.[15–17] This comes as a consequence of the approximate Hamiltonian used in the latter simulations, where the quasi-spherical structure of the micelle was provided by constraining harmonic forces acting on the single-site head

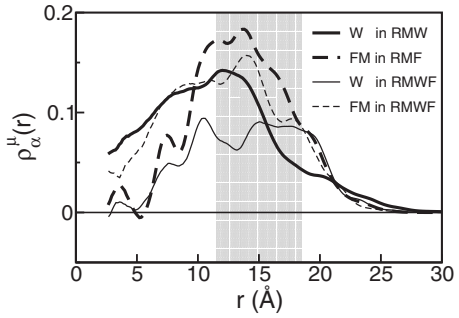

FIG. 3. Local polarization densities for water and formamide species along the radial direction. Different line styles correspond to different systems, as indicated. The shaded area of width 6 Å and centered at $r=15$ Å, corresponds to the interfacial micellar region.

groups. Moreover, this artificial confining potential also induces a larger extent of water structuration around the PHGs which is absent in the present case.

We also investigated the characteristics of the local polarization fluctuations along radial directions. To that end, we analyzed the following correlation function:

$$\rho_\alpha^\mu(r) = \frac{1}{4\pi r^2 \rho_\alpha^{\text{bulk}}} \sum_i \langle \delta(|\mathbf{r}_i^\alpha - \boldsymbol{R}_{\text{c.m.}}| - r)\cos\,\theta_i^\alpha \rangle, \tag{7}$$

where θ_i^α is the angle subtended by the dipole of the ith molecule of species α and the radial vector $\mathbf{r}_i^\alpha - \boldsymbol{R}_{\text{c.m.}}$. Figure 3 displays the polarization densities for water and formamide for the three reverse micelles.

The distributions of dipole orientation exhibit steady growths as one moves from the micellar center toward the polar-phase/head group interface; this feature is much more marked for the RMF case (thick dashed line) than for the RMW one (thick solid line). This somewhat higher degree of orientational correlation of formamide persists in RMWF (thin dashed line); in fact, the polarization of the water molecules in the interior of this micelle drops substantially (thin solid line). In all cases, the corresponding maxima are located at $r\sim 12-13$ Å, where the enhancement of the local polarization reflects the response of the solvent molecules to the strong electric field created by the head groups.

We now move to the analysis of a few relevant site-site spatial correlations. We will start by considering the ion-solvent cases, as described by Na–O and S–O pair distribution functions. Figure 4 shows the local oxygen densities around sodium and sulfur sites for the three micelles.

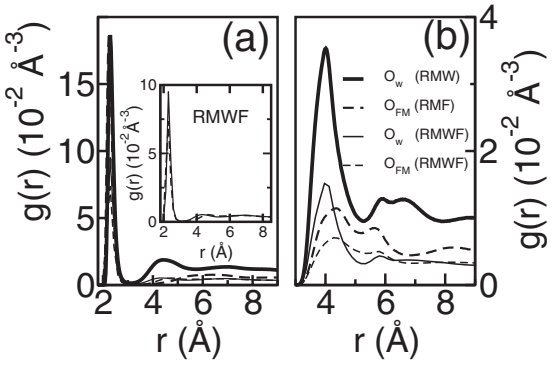

FIG. 4. Local density functions for (a) Na–O and (b) S–O pairs in micelles. Different line styles correspond to different systems, as indicated. An inset has been included in panel (a) for a better visualization of the Na–O data corresponding to the RMWF system.

TABLE III. First solvation shell coordination numbers around sodium and sulfur atoms in micelles.

			RMWF	
Pair	RMW	RMF	O_W	O_{FM}
Na–O	3.40	3.29	1.84	1.58
S–O	8.61	3.92	3.66	2.78

The solvation of Na^+ is characterized in all cases by prominent peaks located at 2.3 Å. The entries shown in Table III reveal that, for pure micelles, the number of oxygen sites comprising the Na^+ first solvation shells are similar: ~3.4 (RMW) and ~3.3 (RMF). The Na^+ coordination numbers in mixed RMWF fall practically to half their corresponding RMW and RMF values.

In RMWF, our simulations indicate a slight preferential solvation of the sodium cations by water [coordination numbers: 1.84 (water) versus 1.58 (formamide)], whereas in bulk equimolar mixtures, dilute Na^+ ions are found to be preferentially solvated by formamide.[58,59] Such a discrepancy may be attributed to the combined effects from the differences in the ionic concentrations and the confinement prevailing in the micellar environment. For example, the presence of large concentrations of ionic species will surely modify the characteristics of the solvent-site density fields around each specific solute species present in the multicomponent inner micellar environment; at the same time, confinement effects would also prevent long wavelength concentration fluctuations (i.e., those longer than the typical size of the micelle roughly given by $\sim R_g$) which, in turn, would give rise to solute-solvent and solvent-solvent spatial correlations different from those observed in macroscopic bulk phases. Incidentally, this result is consistent with the solvent density profiles discussed above which shows that formamide in RMWF tends to be located near the center of the micelle and away

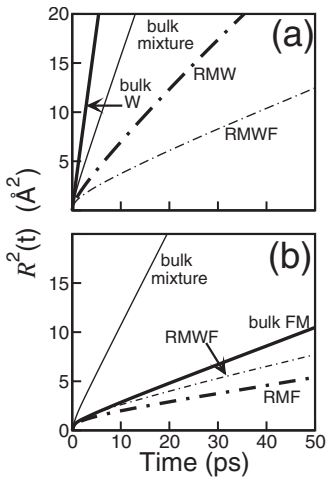

FIG. 5. Mean-squared center-of-mass displacement vs time for (a) water and (b) formamide species in different environments: RMW, RMF, RMWF, bulk water, bulk formamide, and the equimolar bulk solution of W and FM.

TABLE IV. Effective self-diffusion coefficients (10^{-5} cm^2/s) and reorientational times (ps) of water and formamide species in simulated micellar environments.

Species	System	D_{eff}	D_{eff}/D_{bulk}	τ	τ/τ_{bulk}
Water	RMW	0.91	0.15	98.5	48.0
	RMWF	0.36	0.15	207.1	44.5
Formamide	RMF	0.16	0.47	778.3	39.0
	RMWF	0.20	0.12	328.7	49.0

from the highly polar ionic interface. Similarly, information about the solvation of the surfactant polar groups can be extracted from the profiles depicted in Fig. 4(b), which shows correlations involving the head group sulfur and solvent oxygen atoms. The magnitude of the first peak—and consequently the population of the first solvation shell—is larger for RMW (~8.6 molecules). Differences in the molecular sizes of water and formamide may account for the drastic reduction (a factor of 2 approximately) in the population of the first solvation shell of S in RMF. For mixtures, the composition of the sulfur first solvation shell is much closer to being equimolar [3.66 (W) versus 2.78 (FM)] and remains comparable to what we observed for the cation cases.

IV. DYNAMICAL PROPERTIES

The molecular translational mobility of the different species in the polar core can be conveniently described in terms of the time evolution of the mean-squared center-of-mass displacement,

$$\mathcal{R}^2(t) = \langle |\mathbf{r}_i(t) - \mathbf{r}_i(0)|^2 \rangle. \tag{8}$$

Using the classical Einstein expression,[60] an effective diffusion coefficient D_{eff} can be extracted from the linear regime that $\mathcal{R}^2(t)$ exhibits, after an initial inertial transient.[61] The results for $\mathcal{R}^2(t)$ are shown in the two panels of Fig. 5 and the corresponding values of D_{eff} are listed in Table IV.

In the top panel we display the results for water diffusion. Note that the confinement promotes a sharp drop (practically, a factor of ~6) in the translational mobility of water in both RMW and RMWF. Interestingly, the quantitative trends observed in bulk solutions for the implemented Hamiltonian, namely, water diffuses approximately three times slower in equimolar mixtures than in the pure phase, are also reasonably well reproduced in the simulated micellar environments as well. On the other hand, for formamide, confinement effects lead to less drastic reductions in the mobility (a factor of ~2 in RMF); also note that the additional presence of water promotes a much milder acceleration of formamide than the one observed in the bulk. That is, the simulated formamide diffusion coefficient in bulk phases jumps from 0.34×10^{-5} cm^2/s in the pure solvent to 1.66×10^{-5} cm^2/s in an equimolar aqueous mixture, whereas in the micellar environments D_{eff} goes from 0.16×10^{-5} cm^2/s in RMF to 0.20×10^{-5} cm^2/s in RMWF.

We also analyzed the orientational relaxation dynamics by computing the correlation functions:

$$C_\mu^\alpha(t) = \langle P_1[\hat{\mathbf{u}}_i^\alpha(0)\cdot\hat{\mathbf{u}}_i^\alpha(t)]\rangle, \tag{9}$$

where $P_1(x)=x$ is the first-order Legendre polynomial and $\hat{\mathbf{u}}_i^\alpha(t)$ represents a unit vector along the direction of the dipolar moment of the tagged molecule of species α. In Fig. 6, we display the results for $C_\mu^W(t)$ and $C_\mu^{FM}(t)$ in the bulk and in reverse micelles. For micellar environments, one can clearly see that the initial transient time required for the correlation functions to exhibit single-exponential decays may extend up to 50 ps or even longer (Fig. 6). These time scales should be compared to those found in bulk, which are of the order of 1–2 ps, even for the slowest species (FM). In order to obtain a qualitative estimate of the overall retardation that occurs in

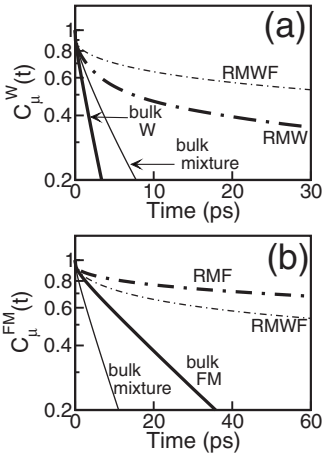

FIG. 6. Single-dipole time correlation function, $C_\mu^\alpha(t)$, for (a) water species and (b) formamide species in reverse micelles and bulk systems. Note the different time scales on (a) and (b) panels.

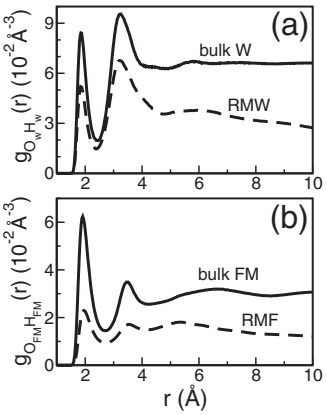

FIG. 7. Radial pair correlation functions for the O–H pairs of (a) water and (b) formamide species obtained for the micellar systems RMW and RMF. The results for corresponding bulk phases are also displayed for comparison.

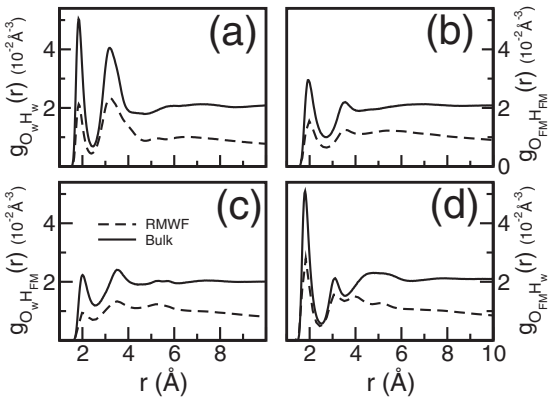

FIG. 8. Radial pair correlation functions for the cross O_i-H_j bonds between water and formamide obtained for the micellar system RMWF. Subindices i and j correspond to water (W) or formamide (FM) species. The corresponding results for the bulk equimolar mixture are also depicted for comparison.

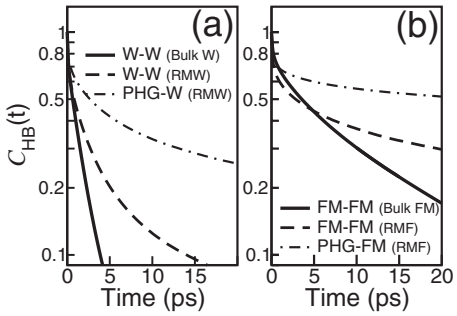

FIG. 9. Survival probability function, $C_{HB}(t)$, for H bonds in (a) RMW and (b) RMF systems, respectively. The curves corresponding to H bonds between the surfactant's PHGs and the polar solvent molecules are also shown. For comparison, the survival probability functions computed in the pure bulk phases are also displayed.

the micelles, we present results for τ, the time integral of $C_\mu(t)$ (Table IV). In doing so, we assumed that the post-librational regimes of all time correlation functions are reasonably well described by biexponential decays. Note that the characteristic reorientational times are a factor of ~40–50 times longer than the corresponding bulk values. As such, the rotational slowing down of water and formamide in the micellar environments is strikingly more pronounced than the translational hindrance (in all cases, the values of D_{eff} are between 2 and 8 times smaller than D_{bulk}).

V. HYDROGEN BOND DYNAMICS

The final aspect that we will examine is the hydrogen bonding (HB) dynamics. Before doing so, we will briefly analyze the equilibrium structures. Perhaps the simplest way to assess the modifications operated in the solvent intermolecular connectivity induced by the micellar confinement is to consider the radial pair correlation functions involving polar hydrogen and oxygen sites in W and FM.

The results for RMW and RMF are shown in the top and bottom panels of Fig. 7, while those for mixed micelles are depicted in Fig. 8. The results reveal that the combined effects of the micellar confinement and the presence of a non-negligible amount of ionic species lead to drastic reductions in the main peak intensities relative to those of the bulk. Peak positions are unaffected, as expected. The corresponding areas under the main peaks located at $r \sim 2$ Å give the OH coordination numbers which are intermediate between 0.4 and 0.6 times those computed in the corresponding bulk phases (Table V).

To investigate the dynamics of HB network within the inner pool and the surface of the micelles, we computed the following time correlation function:

$$C_{HB}(t) = \sum_{ij} \frac{\langle \eta_{ij}(t)\,\eta_{ij}(0)\rangle}{\langle \eta_{ij}^2 \rangle}, \tag{10}$$

where $\eta_{ij}(t)=1$ if molecules i and j are H bonded at time t and zero otherwise, in the intermittent approximation.[50,62–64] For the definition of HB we use the geometrical criterion described in Ref. 50. We considered the hydrogen bonds between solvent molecules and between the surfactant's polar head groups (PHGs) and the solvent species as well. The results for $C_{HB}(t)$ are shown in Fig. 9 for RMW and RMF systems and Fig. 10 shows the HB survival probability for different pairs in the mixed reverse micelle, RMWF.

The estimates for the characteristic times extracted from the time integrals of the normalized correlations functions are listed in Table VI.

As a general observation, we see, in all micellar cases, that the long time decays are not single exponentials, a feature that is also well documented in the bulk phases.[65–68] Concerning the characteristic times corresponding to H bonds between solvent molecules, the qualitative trends observed in the bulk are preserved in micellar environments, although in all cases, the H-bond dynamics in the micelles are between three and four times slower than in the bulk. Moreover, we also remark that HB dynamics in W (FM) remains slower (faster) in mixtures compared to the corresponding neat phases, which is accordant with the trends observed for the self-diffusion coefficients and the reorientational times. Nevertheless, the enhancement in the intermittent H-bond lifetimes as one goes from the bulk to micelles is much less pronounced than the corresponding rise in the

TABLE V. OH first shell coordination numbers.

Pair	RMW	Bulk W	RMF	Bulk FM	RMWF	Bulk mixt.
O_WH_W	1.20	1.82			0.40	0.96
$O_{FM}H_{FM}$			0.92	1.90	0.64	1.10
O_WH_{FM}					0.30	0.80
$O_{FM}H_W$					0.60	1.02

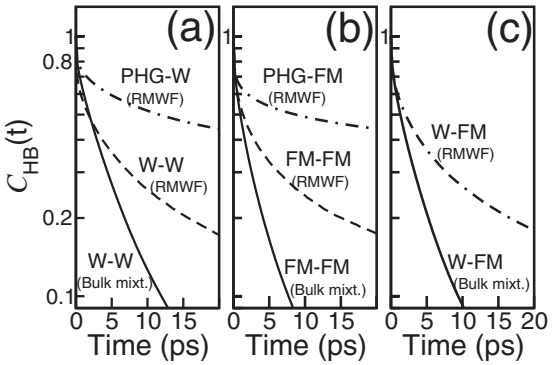

FIG. 10. Survival probability function, $C_{HB}(t)$, for H bonds in the RMWF system, corresponding to (a) water-water and PHG-water pairs, (b) FM-FM and PHG-FM pairs, and (c) water-FM hydrogen bonds. For comparison, the survival probability functions of the corresponding molecular pairs, computed in the pure bulk phases, are also shown.

reorientational characteristic times τ. Most likely, this disparity can be rationalized by considering that a substantial fraction of solvent molecules are coupled to the ionic species in the vicinity of the PHGs instead of participating in solvent-solvent H bonding. These molecules, in turn, would largely contribute to the slowest component of the rotational relaxation but not to the solvent-solvent H-bond dynamics considered. To bring support to this hypothesis, we also computed $C_{HB}(t)$ functions for the PHG-water and PHG-formamide pairs. The results are also displayed in Figs. 9 and 10, whereas the characteristic time scales are presented in the last two columns of Table VI. Note that these HB lifetimes are at least one order of magnitude longer than those describing intermolecular hydrogen bonds between solvent species in the same micellar environment. In passing, we remark that similar trends for the HB lifetimes have been reported by Balasubramanian *et al.*[69] in their study of the slow relaxation of water at the surface of cesium pentadecafluorooctanoate direct micelles. Finally, also note that the results for HB between PHG and the different solvent components in mixtures follow the same trends as those already found for the solvent-solvent connectivity: water-water hydrogen bonds get stronger while HB between formamide species get weakened with the addition of the other solvent component.

VI. SUMMARY

The results presented in this paper provide new insights about the microscopic structures of polar phases in the inner pools of aqueous formamide and mixed water-formamide reversed micelles in bulk cyclohexane and stabilized by the surfactant sodium-AOT. In the range of w_0 investigated—between 4.3 and 7—all micelles adopt ellipsoidal shapes, with linear dimensions of ~15–20 Å and eccentricities varying between 0.7 and 0.8.

The analysis of the local densities of the different components with respect to the centers of mass of the moieties reveals that the inner-pool/surfactant interfaces are considerably irregular, with characteristic roughness lengths comparable to the average micelle radii. Moreover, the effective widths of the surfactant intermediate layers separating the polar and the non-polar phases are much smaller than the characteristic end-to-end distance of a fully stretched AOT molecule. Concerning the characteristics of the local densities of the different components present in the inner pools, two important observations arises: First, a sizable portion—close to 90%—of the Na^+ ions remains tightly bound to the head groups. Second, in mixed micelles, the central part of the inner pool shows a moderate enhancement of the local concentration of formamide, in detriment of water. Formamide also exhibits a larger extent of dipole orientation polarization induced by the strong electric fields generated by the head groups, which results in an overall dipolar alignment pointing radially outward. Interestingly, the combined effects of the spatial confinement and the presence of large ionic concentration from head groups and Na^+ counterions change the preferential solvation of the sodium ions with respect to the bulk equimolar mixture. In RMWF, Na^+ is slightly preferentially hydrated, whereas the opposite behavior is found in bulk equimolar mixtures containing diluted Na^+ ions.

Concerning the dynamical characteristics of the polar solvents, we observed drastic increments in the characteristic time scales describing the translational and rotational motions of the two solvents. Changes in the translational diffusion characteristics are more marked in water, where the ratio between the corresponding bulk and micelle diffusion coefficients is ~6. Similar to what is observed in the bulk phases, formamide molecules move faster in the presence of water than in the single-component phase, and the observed differences are enhanced by the spatial confinement prevailing within the micellar environment. Differences in the dynamical behavior are even much more dramatic in the rotational dynamics, where the characteristic times describing

TABLE VI. Average H-bond intermittent lifetimes (in ps) for water-water, formamide-formamide, water-formamide, surfactant's PHGs-water, and PHG-formamide pairs, calculated as time integrals of the corresponding survival probability function $C_{HB}(t)$.

System	τ_{HB}^{WW}	$\tau_{HB}^{FM\ FM}$	$\tau_{HB}^{W\ FM}$	$\tau_{HB}^{PHG\ W}$	$\tau_{HB}^{PHG\ FM}$
			Bulk		
Water	1.51	···	···		
Formamide	···	8.24	···		
Mixture 1:1	3.90	3.16	2.63		
			Reverse micelles		
RMW	5.37	···	···	43.4	···
RMF	···	23.05	···	···	279.0
RMWF	10.83	11.28	11.19	146.3	191.8

the orientational relaxation of the two solvents in micelles are a factor of ~40–50 larger compared with bulk results.

The characteristics of the intramolecular connectivity expressed in terms of the number of hydrogen bonds show a drastic reduction; in the micellar sizes investigated only one-half of the hydrogen bonds originally found in the corresponding bulk phases remains in the micelles. From the dynamical perspective, the average lifetime of the overall hydrogen bond dynamics in micelles is approximately three to four times larger than that of the bulk. The mismatch between the rotational relaxation retardation (~50-fold) and the solvent-solvent H-bond lifetime enhancement (~4-fold) observed in going from bulk to micellar inner pools are likely to arise from the largely immobilized solvent molecules located near the polar interfaces, which do not contribute to solvent-solvent H-bond dynamics.

ACKNOWLEDGMENTS

D.L and M.D.E are members of Carrera de Investigador Científico de CONICET (Argentina). M.H.H.P acknowledges financial support from CONICET (Argentina). M.S.S thanks Fapesp and CNPq for financial support.

[1] T. P. Hoar and J. H. Schulman, Nature (London) **152**, 102 (1943).
[2] N. E. Levinger, Science **298**, 1722 (2002).
[3] J. Lang, A. Jada, and A. Malliaris, J. Phys. Chem. **92**, 1946 (1988).
[4] J. J. Silber, A. Biasutti, E. Abuin, and E. Lissi, Adv. Colloid Interface Sci. **82**, 189 (1999).
[5] A. Maitra, J. Phys. Chem. **88**, 5122 (1984).
[6] H. Hauser, G. Haering, A. Pande, and P. L. Luisi, J. Phys. Chem. **93**, 7869 (1989).
[7] B. Baruah, J. M. Roden, M. Sedgwick, N. M. Correa, D. C. Crans, and N. E. Levinger, J. Am. Chem. Soc. **128**, 12758 (2006).
[8] M. Kotlarchyk and J. S. Huang, J. Phys. Chem. **89**, 4382 (1985).
[9] A. Amararene, M. Gindre, J.-Y. Le Huérou, W. Urbach, D. Valdez, and M. Waks, Phys. Rev. E **61**, 682 (2000).
[10] M. R. Harpham, B. M. Ladanyi, and N. E. Levinger, J. Chem. Phys. **121**, 7855 (2004).
[11] J. Zhang, B. Han, J. Liu, X. Zhang, G. Yang, J. He, Z. Liu, T. Jiang, J. Wang, and B. Dong, J. Chem. Phys. **118**, 3329 (2003).
[12] D. S. Venables, K. Huang, and C. A. Schmuttenmaer, J. Phys. Chem. B **105**, 9132 (2001).
[13] I. R. Piletic, D. E. Moilanen, D. B. Spry, N. E. Levinger, and M. D. Fayer, J. Phys. Chem. A **110**, 4985 (2006).
[14] J. E. Boyd, A. Briskman, C. M. Sayes, D. Mittleman, and V. Colvin, J. Phys. Chem. B **106**, 6346 (2002).
[15] J. Faeder and B. M. Ladanyi, J. Phys. Chem. B **104**, 1033 (2000).
[16] J. Faeder and B. M. Ladanyi, J. Phys. Chem. B **105**, 11148 (2001).
[17] J. Faeder and B. M. Ladanyi, J. Phys. Chem. B **109**, 6732 (2005).
[18] D. Laria and R. Kapral, J. Chem. Phys. **117**, 7712 (2002).
[19] D. J. Tobias and M. L. Klein, J. Phys. Chem. **100**, 6637 (1996).
[20] S. Senapati and M. L. Berkowitz, J. Phys. Chem. B **107**, 12906 (2003).
[21] S. Senapati and M. L. Berkowitz, J. Chem. Phys. **118**, 1937 (2003).
[22] S. Salaniwal, S. T. Cui, P. T. Cummings, and H. D. Cochran, Langmuir **15**, 5188 (1999).
[23] S. Abel, F. Sterpone, S. Bandyopadhyay, and M. Marchi, J. Phys. Chem. B **108**, 19458 (2004).
[24] S. Abel, M. Waks, M. Marchi, and W. Urbach, Langmuir **22**, 9112 (2006).
[25] R. Allen, S. Bandyopadhyay, and M. L. Klein, Langmuir **16**, 10547 (2000).
[26] J. Rodriguez, J. Martí, E. Guàrdia, and D. Laria, J. Phys. Chem. B **111**, 4432 (2007).
[27] M. R. Harpham, B. M. Ladanyi, and N. E. Levinger, J. Phys. Chem. B **109**, 16891 (2005).
[28] J. Faeder, M. V. Albert, and B. M. Ladanyi, Langmuir **19**, 2514 (2003).
[29] S. Pal, S. Balasubramanian, and B. Bagchi, Phys. Rev. E **67**, 061502 (2003).
[30] S. Pal, S. Balasubramanian, and B. Bagchi, J. Phys. Chem. B **107**, 5194 (2003).
[31] S. Pal, S. Balasubramanian, and B. Bagchi, J. Chem. Phys. **117**, 2852 (2002).
[32] I. Rico and A. Lattes, J. Colloid Interface Sci. **102**, 285 (1984).
[33] S. E. Friberg and M. Podzinsek, Colloid Polym. Sci. **262**, 252 (1984).
[34] P. D. I. Fletcher, M. F. Galal, and B. H. Robinson, J. Chem. Soc., Faraday Trans. 1 **80**, 3307 (1984).
[35] R. E. Riter, E. P. Undiks, J. R. Kimmel, and N. E. Levinger, J. Phys. Chem. B **102**, 7931 (1998).
[36] H. Shirota and H. Segawa, Langmuir **20**, 329 (2004).
[37] S. K. Pal, D. Mandal, D. Sukul, and K. Bhattacharyya, Chem. Phys. Lett. **312**, 178 (1999).
[38] R. E. Riter, E. P. Undiks, and N. E. Levinger, J. Am. Chem. Soc. **120**, 6062 (1998).
[39] C. A. T. Laia, W. Brown, M. Almgren, and S. M. B. Costa, Langmuir **16**, 8763 (2000).
[40] N. M. Correa, P. A. R. Pires, J. J. Silber, and O. A. El Seoud, J. Phys. Chem. B **109**, 21209 (2005).
[41] O. F. Nielsen and P. A. Lund, Chem. Phys. Lett. **78**, 626 (1981).
[42] Y. J. Chang and E. W. Castner, Jr., J. Chem. Phys. **99**, 113 (1993).
[43] M. C. Bellissent-Funel, S. Nasr, and L. Bosio, J. Chem. Phys. **106**, 7913 (1997).
[44] H. Ohtaki, J. Mol. Liq. **103–104**, 3 (2003).
[45] W. L. Jorgensen and C. J. Swenson, J. Am. Chem. Soc. **107**, 569 (1985).
[46] W. L. Jorgensen and C. J. Swenson, J. Am. Chem. Soc. **107**, 1489 (1985).
[47] K. P. Sagarik and R. Ahlrichs, J. Chem. Phys. **86**, 5117 (1987).
[48] Y. P. Puhovski and B. M. Rode, Chem. Phys. **190**, 61 (1995).
[49] E. Tsuchida, J. Chem. Phys. **121**, 4740 (2004).
[50] M. D. Elola and B. M. Ladanyi, J. Chem. Phys. **125**, 184506 (2006).
[51] C. de Visser, W. J. M. Heuvelsland, L. A. Dunn, and G. Somsen, J. Chem. Soc., Faraday Trans. 1 **74**, 1159 (1978).
[52] J. A. D. MacKerell, N. Banavali, and N. Foloppe, Biopolymers **56**, 257 (2000).
[53] W. L. Jorgensen, J. Chandrasekhar, J. Madura, R. W. Impey, and M. L. Klein, J. Chem. Phys. **79**, 926 (1983).
[54] L. D. Schuler, X. Daura, and W. F. van Gunsteren, J. Comput. Chem. **22**, 1205 (2001).
[55] W. F. van Gunsteren, S. R. Billeter, A. A. Eising, P. H. Hünenberger, P. Krüger, A. E. Mark, W. R. P. Scott, and I. G. Tironi, *Biomolecular Simulation: The GROMOS96 Manual and User Guide* (vdf Hochschulverlag AG an der ETH Zürich and BIOMOS b.v, Zürich, Groningen, 1996).
[56] G. Milano and F. Müller-Plathe, J. Phys. Chem. B **108**, 7415 (2004).
[57] J. C. Phillips, R. Braun, W. Wang, J. Gumbart, E. Tajkhorshid, E. Villa, C. Chipot, R. D. Skeel, L. Kale, and K. Schulten, J. Comput. Chem. **26**, 1781 (2005).
[58] Y. P. Puhovski and B. M. Rode, Chem. Phys. **222**, 43 (1997).
[59] C. K. Finter and H. G. Hertz, Z. Phys. Chem., Neue Folge **148**, 75 (1986).
[60] M. P. Allen and D. J. Tildesley, *Computer Simulation of Liquids* (Oxford University Press, New York, 1994).
[61] The effective diffusion coefficient D_{eff} computed for water and formamide in the micellar interior accounts for translational motions within a time scale which is small compared to that characterizing the diffusion of the micelle center of mass in cylcohexane.
[62] J. Martí, J. A. Padró, and E. Guàrdia, J. Chem. Phys. **105**, 639 (1996).
[63] A. Luzar, J. Chem. Phys. **113**, 10663 (2000).
[64] E. Guàrdia, D. Laria, and J. Martí, J. Phys. Chem. B **110**, 6332 (2006).
[65] D. A. Zichi and P. J. Rossky, J. Chem. Phys. **84**, 2814 (1986).
[66] F. Sciortino, P. H. Poole, H. E. Stanley, and S. Havlin, Phys. Rev. Lett. **64**, 1686 (1990).
[67] A. C. Belch and S. A. Rice, J. Chem. Phys. **86**, 5676 (1987).
[68] A. Luzar and D. Chandler, Nature (London) **379**, 55 (1996).
[69] S. Balasubramanian, S. Pal, and B. Bagchi, Phys. Rev. Lett. **89**, 115505 (2002).